Cassegrain system," M.I.T. Lincoln Lab., Lexington, Mass., Tech. Rep. 484, ESD-TR-71-271, Sept. 24, 1971.
[3] ——, "Limited electronic scanning with an offset-feed near-field Gregorian system," M.I.T. Lincoln Lab., Lexington, Mass., Tech. Rep. 486, ESD-TR-272, Sept. 24, 1971.
[4] C. J. Miller and D. Davis, "LFOV optimization study final report" ESD-TR-72-102, Jan. 1972.
[5] W. T. Patton, "Analysis of radar electronic scan technique (REST)," Deputy for Engineering and Technology, Electronic Systems Division, A. F. Systems Command, L. G. Hanscom Field, Bedford, Mass., Tech. Rep. ESD-TR-66-355.
[6] R. Tang, "Survey of time-delay beam steering techniques," in *1970 Progr. and Dig. Phased-Array Antenna Symp.*, pp. 93–96.
[7] R. J. Mailloux, "Array techniques for limited scan application," U.S.A.F. Cambridge Res. Lab., Bedford, Mass., Physical Sci. Res. Papers 503, Project 4600, AFCRL-72-0421, July 19, 1972.
[8] R. J. Mailloux, P. R. Caron, F. J. LaRussa, and C. L. Dunne, "Phase interpolation circuits for scanning phased arrays," NASA Tech. Note TN D-5865, July 1970.
[9] G. N. Tsandoulas and W. D. Fitzgerald, "Aperture efficiency enhancement in dielectrically loaded horns," *IEEE Trans. Antennas Propagat.*, vol. AP-20, pp. 69–74, Jan. 1972.

Near Fields of Wire Antennas by Matrix Methods

ARLON T. ADAMS, BRADLEY J. STRAIT, DANIEL E. WARREN, DAH-CHENG KUO, AND THOMAS E. BALDWIN, JR.

Abstract—**The method of moments [1], [2] is applied to wire antenna near-field problems. Within the general method, two computational procedures are developed. Results of these are compared with those of certain approximate analytical techniques and also with those of other investigators. A treatment for junctions is outlined. Examples are included for a single dipole antenna, for linear arrays of dipoles and also for loop and T-junction radiators.**

I. Introduction

THE MATRIX methods originally suggested by Harrington [1], [2] have been used to treat a variety of practical problems of electromagnetic engineering interest. As one particular application, these methods have served for analysis and design of radiation and scattering systems consisting of arbitrarily bent and interconnected thin wires [3]–[6]. It has been shown that for analysis problems, it is possible to compute accurately the current distribution of a given wire structure as well as input impedances corresponding to feed points and any far-field radiation or scattering patterns of interest. The purpose of this paper is to show how matrix methods can be extended and used for computation of near-field distributions as well.

The methods suggested in this paper can be used to compute near fields of arbitrary configurations of thin wires that can be excited or loaded at arbitrary points along their lengths. It is only necessary to specify the problem geometry completely including the exact positions of any applied excitations and loads. It is possible to include wire junctions in the problem enabling treatment of certain special configurations of practical interest such as crossed wires, supporting wires for long antennas, and so on. The restriction to thin wires implies that each wire length L and radius a are such that $L/a \gg 1$ and $a \ll \lambda$, the wavelength.

Several examples are included here to illustrate use of the matrix methods suggested. Typical results are presented and compared with those of other investigators. These results were computed with user-oriented computer programs written especially for practicing engineers and which are now on deposit and easily obtained [7], [8].

Manuscript received September 28, 1972; revised March 5, 1973. This work was supported in part by the Rome Air Development Center, Griffis AFB, Rome, N. Y., under Contract AF30(602)2636 and in part by the Air Force Cambridge Research Laboratories, Air Force Systems Command, under Contract F19628-68-C-0180, and pursued under Rome Air Development Center Post-Doctoral Program in cooperation with Syracuse University under Contract F30602-70-C-0086 and in cooperation with the Atlantic Research Corporation under Contracts F30602-69-C-0047, F30602-69-C-0051, and F30602-71-C-0358.

A. T. Adams, B. J. Strait, D. E. Warren, and D. C. Kuo are with the Department of Electrical and Computer Engineering, Syracuse University, Syracuse, N. Y. 13210.
T. E. Baldwin, Jr., is with the Advanced Projects Group, Atlantic Research Corporation, Alexandria, Va.

II. Near-Field Calculations

The details of Harrington's general method of analysis are available elsewhere [1], [2]. It is assumed here the wires are thin and that current flows only in the axial direction of each. Current and charge densities are approximated by filaments of current and charge on the wire axes. The boundary condition regarding the tangential component of the electric field at the wire surfaces is satisfied (approximately) by requiring that the axial component vanish at the surface of each wire. In the subsectional approach used each wire is thought of as divided into a number of short segments or subsections connected together. A generalized impedance matrix $[Z]$ is then obtained using the method of moments to describe the electromagnetic interactions between subsections. In the process the integro-differential equation characterizing the problem is reduced to a matrix equation of the form

$$[V] = [Z][I]. \tag{1}$$

Authorized licensed use limited to: INDIAN INSTITUTE OF TECHNOLOGY KHARAGPUR. Downloaded on May 06,2023 at 05:35:48 UTC from IEEE Xplore. Restrictions apply.

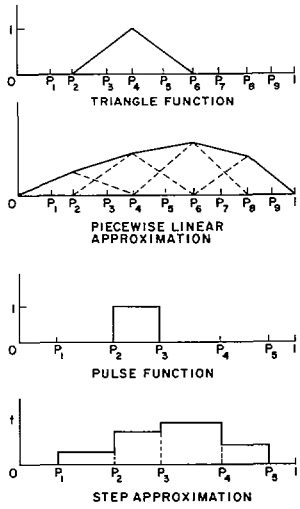

Fig. 1. Subsectional bases and functional approximation.

This is done by expanding the current of the wire structure in a sequence of subsectional expansion functions where each is nonzero only over a small portion of a wire; that is, over a small number of subsections. Of the many possible choices for sets of expansion functions only two are used in this work. These are the triangle functions shown in Fig. 1(a) which result in a piecewise linear approximation (Fig. 1(b)) to the current and the pulse functions of Fig. 1(c) which result in a step approximation (Fig. 1(d)). The elements of the column matrix $[I]$ are simply complex numbers representing the amplitudes of the corresponding current expansion functions, and the elements of $[V]$ are related to the excitation of the wire structure.

The usual analysis problems are considered solved once a well-conditioned impedance matrix $[Z]$ has been obtained. Given a set of excitation voltages the current matrix is obtained by inverting $[Z]$, normally a simple task for modern high-speed computers. Once the current is known the input impedances corresponding to feed points and various far-field patterns of interest can be calculated using standard formulas in the usual way [3], [9], [10]. An additional step or procedure is required, however, for computations of most near-field distributions. This paper describes two such procedures, both stemming from (1), that have been programmed. The computer programs have been carefully written, studied, and debugged by cross-checking results and, as mentioned earlier, they are both readily available in user-oriented form.

A. Procedure Based on Reciprocity (Method 1)

It is assumed in this discussion that the current distribution has been computed for a given problem using the method of moments so that the current matrix $[I]$ is known. By the reciprocity theorem

$$\int_v \boldsymbol{E}_1 \cdot \boldsymbol{J}_2 \, dv = \int_v \boldsymbol{E}_2 \cdot \boldsymbol{J}_1 \, dv \tag{2}$$

where $\boldsymbol{J}_1$ and $\boldsymbol{J}_2$ are source current densities, and $\boldsymbol{E}_1$ and $\boldsymbol{E}_2$ are the corresponding electric fields. It is convenient to consider $\boldsymbol{J}_1$ as the known current on the structure and $\boldsymbol{J}_2$ as the current of an infinitesimal testing dipole placed at the field point in question and oriented with the desired field component. It is assumed that the current of each wire flows only in its axial direction. If l_1 denotes the wire structure and l_2 the testing dipole then (2) can be written as

$$\int_{l_2} \boldsymbol{E}_1 \cdot \boldsymbol{I}_2 \, d\boldsymbol{l}_2 = \int_{l_1} \boldsymbol{E}_2 \cdot \boldsymbol{I}_1 \, d\boldsymbol{l}_1 \tag{3}$$

where I_1 and I_2 are axial currents with directions indicated by $d\boldsymbol{l}_1$ and $d\boldsymbol{l}_2$, respectively. For the infinitesimal dipole I_2 is thought of as constant over l_2 as $l_2 \to 0$. Thus (3) becomes

$$(E_1)_{\text{along } l_2} = \frac{1}{I_2 l_2} \int_{l_1} \boldsymbol{E}_2 \cdot \boldsymbol{I}_1 \, d\boldsymbol{l}_1 \tag{4}$$

The current I_1 is known and $\boldsymbol{E}_2$, the field of the infinitesimal dipole, can be calculated easily. Hence, (4) is a useful starting point from which the desired field components can be found.

$\boldsymbol{E}_2$ can be calculated using the vector and scalar potentials as

$$\boldsymbol{E}_2 = -j\omega\mu \boldsymbol{A}_2 - \nabla\phi_2 \tag{5}$$

where [10]

$$\boldsymbol{A}_2 = \frac{I_2 \boldsymbol{l}_2}{4\pi R} \exp(-jkR) \tag{6}$$

$$\phi_2 = -\frac{1}{j\omega\epsilon} \nabla \cdot \boldsymbol{A}_2 = \frac{I_2 \exp(-jkR)}{4\pi j\omega\epsilon R} \left\{ \frac{1}{R} + jk \right\} \boldsymbol{l}_2 \cdot \hat{R} \tag{7}$$

and where $k = 2\pi/\lambda$. R is the distance from the testing dipole to a point on l_1 and $\hat{R}$ is its associated unit vector. Substituting (5) into (4) and integrating by parts yields

$$(E_1)_{\text{along } l_2} = \frac{1}{I_2 l_2} \left\{ -j\omega\mu \int_{l_1} I_1 \boldsymbol{A}_2 \cdot d\boldsymbol{l}_1 + \int_{l_1} \phi_2 \frac{dI_1}{dl_1} dl_1 \right\} \tag{8}$$

where use has been made of the fact that the current vanishes at open ends of wires.

The current expansion selected for use with this procedure is the piecewise linear approximation of Fig. 1(b). (Triangle functions are also used as testing functions resulting in a Galerkin solution. For this choice formulas and subroutines are available for computing $[V]$ and $[Z]$ [3], [5], [9].) In this case the expansion can be written as

$$I_1 = \sum_{n=1}^{N} I_n' T_n \tag{9}$$

Authorized licensed use limited to: INDIAN INSTITUTE OF TECHNOLOGY KHARAGPUR. Downloaded on May 06,2023 at 05:35:48 UTC from IEEE Xplore. Restrictions apply.

where T_n is the nth triangle expansion function, I_n' it is complex amplitude and N is the total number of expansion functions of current. Inserting (9) in (8) results in

$$(E_1)_{\text{along } l_2} = \frac{1}{I_2 l_2}\left\{-j\omega\mu \sum_{n=1}^{N} \int_{l_1} I_n' T_n A_2 \cdot dl_1 + \sum_{n=1}^{N} \int_{l_1} \phi_2 I_n' \frac{dT_n}{dl_1}\, dl_1\right\}. \quad (10)$$

The numerical integrations used to evaluate (10) with (6) and (7) incorporated are somewhat involved and are not discussed here. However, the details are available [4]. At this point then the procedure for computing near fields is straightforward. For example, to calculate the x,y,z components of the electric-field vector at some near-field point it is simply necessary to evaluate (10) three times, once for each coordinate direction. The same is true for any set of components. This procedure is repeated for each field point of interest, and with sufficient data the desired near-field distributions can be plotted. The use of this method is illustrated with comments on convergence in the examples that follow. Programming has been checked by comparing results with those obtained using a second or alternative procedure that will be discussed.

B. Alternative Procedure (Method 2)

If the current of the wire structure in question is approximated using a total of N expansion functions then (1) simply represents

$$\begin{bmatrix} V_1 \\ V_2 \\ \vdots \\ V_N \end{bmatrix} = \begin{bmatrix} z_{11} & z_{12} & \cdots & z_{1N} \\ z_{21} & z_{22} & \cdots & z_{2N} \\ \cdots & \cdots & \cdots & \cdots \\ z_{N1} & z_{N2} & \cdots & z_{NN} \end{bmatrix} \begin{bmatrix} I_1 \\ I_2 \\ \vdots \\ I_N \end{bmatrix}. \quad (11)$$

To test the electric field at a given point in the near field, a small (testing) thin-wire dipole can be placed at the point with its axis parallel to the vector component of interest. An additional expansion function is assumed over this testing wire so that the total is now $(N + 1)$. Now the system is characterized by an expanded Z matrix as

$$\begin{bmatrix} V_1 \\ V_2 \\ \vdots \\ V_{N+1} \end{bmatrix} = \begin{bmatrix} z_{11} & z_{12} & \cdots & z_{1(N+1)} \\ z_{21} & z_{22} & \cdots & z_{2(N+1)} \\ \cdots & \cdots & \cdots & \cdots \\ z_{(N+1)1} & z_{(N+1)2} & \cdots & z_{(N+1)(N+1)} \end{bmatrix} \begin{bmatrix} I_1 \\ I_2 \\ \vdots \\ I_{N+1} \end{bmatrix}. \quad (12)$$

If the testing wire is open-circuited then $I_{N+1} = 0$ so that

$$V_{N+1} = z_{(N+1)1} I_1 + z_{(N+1)2} I_2 + \cdots + z_{(N+1)N} I_N. \quad (13)$$

Knowledge of the current distribution over the wire structure and of an additional row of the impedance matrix representing mutual impedances between the wire structure and the testing dipole enables computation of the open-circuit voltage at the testing port The electric field strength along the direction $\hat{l}$ of the testing wire is given by

$$E_{\text{along } \hat{l}} = \frac{-(V_{N+1}) \text{ open circuit}}{\text{length of testing dipole}}. \quad (14)$$

As before, the procedure for computing near fields is to evaluate (14) once for each electric field vector component of interest (at each point). In passing it should be pointed out that a comparable procedure is available for computing components of the near magnetic field [12]. Though this is not elaborated on here some results are included. It should also be pointed out that a testing dipole of length 0.001λ was used to obtain the results reported here.

It is important to note that with both procedures for calculating near fields the current distribution of the actual antenna is computed in the absence of the testing element used to sample the field. With regard to the second method this means that the impedance matrix shown in (11) is inverted to obtain the antenna current rather than the expanded matrix of (12). The last row of the matrix in (12) is computed and used only to calculate one component of the near field at a particular point. Hence, this row must be recomputed for each component at each point. That near-field results are essentially independent of the particular testing wire used is evident from the absence of the self-impedance term $z_{(N+1)(N+1)}$ from (13).

This alternative procedure has been programmed using the staircase current approximation of Fig. 1(d). (In this case the testing functions are impulses [multiplied by the segment lengths] corresponding to a point-matching solution. Here, again, formulas and subroutines for computing elements of $[V]$ and $[Z]$ are readily available [1], [8], [12].) Results of the two procedures (and programs) discussed here are compared with the examples that follow.

Finally, it should be noted that the two programs (corresponding to methods 1 and 2) will provide essentially identical results (except for some computational inaccuracies) if identical expansion functions and segment lengths are used and if the testing functions used with method 2 are impulses.

C. Wire Loading

There have been two general methods described for including both discrete and distributed wire loading in the method of moments [9], [13], [14]. Hence, it is also possible to compute near fields of loaded thin-wire antennas. It is only necessary to define a load impedance matrix $[Z_L]$ which is added directly to the generalized impedance matrix $[Z]$. Then, regardless of whether $[Z]$ has been computed using triangles or pulses, the current matrix $[I]$ is given by

$$[I] = [[Z] + [Z_L]]^{-1}[V]. \quad (15)$$

Formulas and computational routines are available for obtaining $[Z_L]$ for use with both triangle functions in a Galerkin solution and pulse functions in a point-matching solution [3], [5], [8], [9], [12]. Finally, once the current of the loaded structure has been computed using (15) the

Authorized licensed use limited to: INDIAN INSTITUTE OF TECHNOLOGY KHARAGPUR. Downloaded on May 06,2023 at 05:35:48 UTC from IEEE Xplore. Restrictions apply.

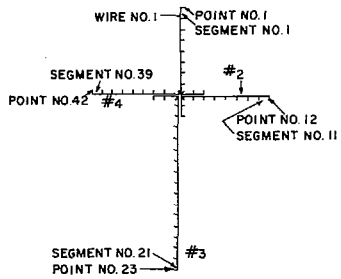

Fig. 2. Thin wire cross treated as four open-ended wires.

near-field computations can proceed as outlined in the preceding.

D. Wire Junctions

It has been shown [3] that when using triangle expansion functions a junction of M wires can be treated as a problem involving M open-ended wires with $M - 1$ overlaps as depicted in Fig. 2 for the case $M = 4$. Here, the wire cross is shown as a junction of four open-ended wires with three overlaps. The geometry of the problem is specified using a total of 42 points (indicated by hatch marks) and the various points and segments are numbered consecutively from the first point and segment of the first wire to the last point and segment of the fourth wire. It is evident that three triangle expansion functions overlap the junction. That is, the fourth triangle overlaps the junction by extending from the seventh point to point 11, while the eighth triangle overlaps from point 18 to point 22, and so on. That the number of overlaps is $M - 1$ rather than M is required to insure an independent set of expansion functions. Solutions obtained by treating problems involving wire junctions in this manner correctly satisfy both Kirchhoff's current law and the continuity of potential condition at each junction. The method has already been used in successful studies of several radiation and scattering problems of interest [3]–[6]. In passing, it should be pointed out that a simple wire loop is treated as a single open-ended wire with one overlap. This is illustrated with the example of the circular loop considered later

Of course, junction problems can also be handled with other sets of expansion functions including pulses. However, most problems to date have been treated with triangles as described before. The pulse solution was discussed in a recent article by Sayre [15] and is not elaborated on here.

III. Checking Near-Field Calculations

In the regions close to the antenna wires, the computed fields may be checked using approximate relationships derived directly from Maxwell's equations. Consider a typical subsection Δl_n of a wire antenna. A local cylindrical coordinate system (ρ_n,ϕ_n,z_n) with unit vectors $(\hat{\rho}_n,\hat{\phi}_n,\hat{z}_n)$ can be employed, where $\hat{\rho}_n$ is normal and $\hat{z}_n$ parallel to the wire over the given subsection. If the wire structure is excited by a voltage V_n' and loaded with an impedance Z_{ln} within Δln then the net voltage V_n across the subsection is $V_n = V_n' - Z_{ln}I_n$ and the tangential field E_{z_n} just outside the subsection is

$$E_{z_n} = \frac{V_n}{\Delta l_n} = \frac{V_n' - Z_{ln}I_n}{\Delta l_n}. \tag{16}$$

The normal component of the electric field at some arbitrary near-field point outside the given subsection is denoted by E_{ρ_n} and is found by constructing a cylinder of radius ρ_n and differential length dl about the wire. Then, Gauss' law yields

$$\text{charge per unit length} = \frac{1}{dl}\oint\!\!\!\!\!\!\diagup_{S} \boldsymbol{D}\cdot\hat{n}\, ds$$

$$\approx 2\pi\rho_n\epsilon E_{\rho_n} + \epsilon \iint_{S_1} \frac{\partial E_{z_n}}{\partial z_n} ds$$

(where S is the total surface of the cylinder and S_1 is one of its end faces). Charge per unit length may be represented as $-(1/j\omega)(\partial I/\partial z_n)$ (using the equation of continuity) and

$$E_{\rho_n} \approx -\frac{1}{j\omega\epsilon}\left(\frac{\partial I}{\partial z_n} + j\omega\epsilon \iint_{S_1} \frac{\partial E_{z_n}}{\partial z_n} ds\right) \Big/ 2\pi\rho_n. \tag{17}$$

Application of Maxwell's second-curl equation yields

$$\oint_c \boldsymbol{H}\cdot d\boldsymbol{l} = I_n + j\omega\epsilon \iint_{S_1} \boldsymbol{E}\cdot\hat{n}\, ds \approx 2\pi\rho_n H_{\phi_n}$$

where contour c is a circle centered on the wire, lying in a constant z_n plane and S_1 is the area of the circle. Then,

$$H_{\phi_n} \approx (I_n + j\omega\epsilon \iint_{S_1} E_{z_n}\, ds)/2\pi\rho_n \tag{18}$$

Note that, for problems with rotational symmetry, (17) and (18) become exact rather than approximate and are related by

$$E_{\rho_n} = -\frac{1}{j\omega\epsilon}\frac{\partial H_{\phi_n}}{\partial z_n}.$$

In some cases the second term of (17) and (18) is negligible. The second term becomes increasingly significant near the ends and gap region of the wire antenna, for high frequencies, and for large ρ_n. Its value exceeds that of the first term in some cases. I_n and $\partial I/\partial z_n$ may be evaluated from computed values of current. E_{z_n} and $\partial E_{z_n}/\partial z_n$ may be evaluated from (16) or computed data. The use of the first terms of (17) and (18) gives a direct check on computed near fields and the use of the second term, where it is significant, provides a check on consistency.

The relationships (17) and (18) are most useful in regions close to the wires. In regions slightly more distant the Hertzian dipole formulas are helpful. That is, an accurate check on near-field results can be obtained by replacing each subsection with one or more Hertzian

Authorized licensed use limited to: INDIAN INSTITUTE OF TECHNOLOGY KHARAGPUR. Downloaded on May 06,2023 at 05:35:48 UTC from IEEE Xplore. Restrictions apply.

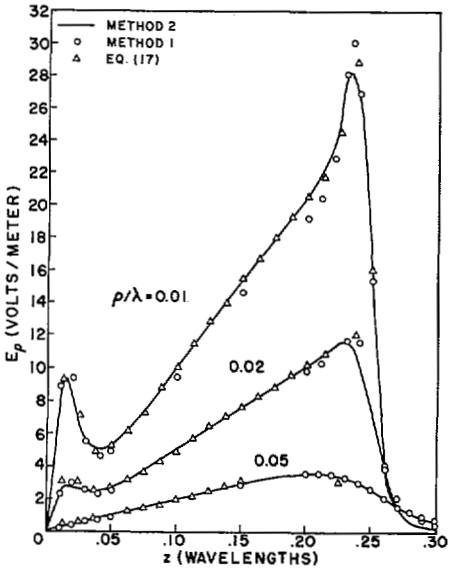

(a)

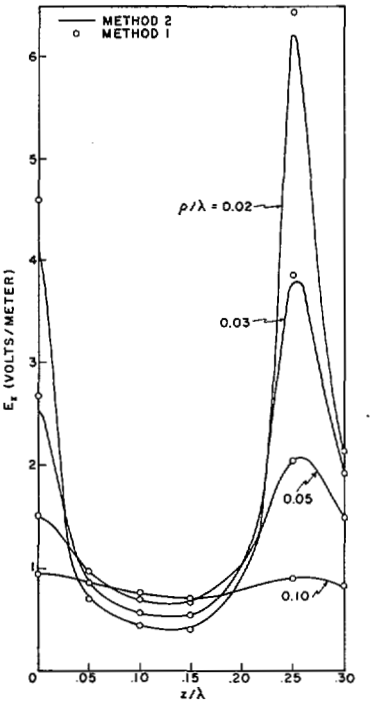

(b)

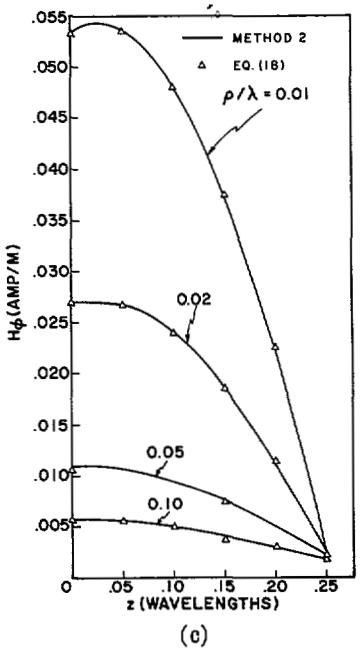

(c)

Fig. 3. Near fields of center-fed half-wave dipole (radius = 0.005λ). (a) E_ρ. (b) E_z. (c) H_ϕ.

dipoles. In this case close agreement is found (within 1 percent) with other computed results for distances greater than 0.2λ from any wire.

IV. Dipoles and Junctions

Fig. 3 shows the computed electric and magnetic near fields of a center-fed half-wavelength dipole of radius 0.005λ. Fields are given in V/m or A/m with an assumed wavelength of 3 m. These results can be compared with those of other investigators [16]–[21]. Note that the radial field E_ρ dominates over most of the region shown. E_ρ has peaks near the gap and ends, with higher peaks at the ends. In the region half-way between the gap and the ends $\partial E_z/\partial z$ is nearly zero and, therefore, E_ρ has approximately a $(1/\rho)$ dependence (see (17)). The crossover of curves for E_ρ between $z = 0.25\lambda$ and 0.30λ can be explained by the fact that E_ρ must be zero on-axis for $|z| > 0.25\lambda$.

The tangential component E_z is small except in the gap region and near the ends of the antenna. The field E_z near

Authorized licensed use limited to: INDIAN INSTITUTE OF TECHNOLOGY KHARAGPUR. Downloaded on May 06,2023 at 05:35:48 UTC from IEEE Xplore. Restrictions apply.

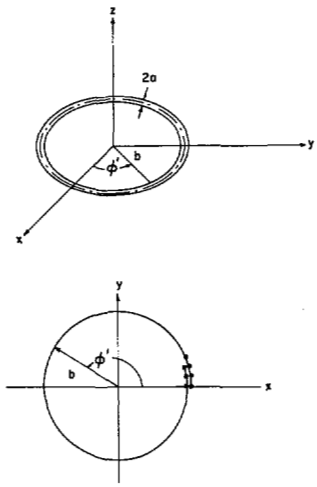

Fig. 4. Circular loop antenna represented by single open-ended wire with two overlapping segments. Excitation is at $\phi' = 0$.

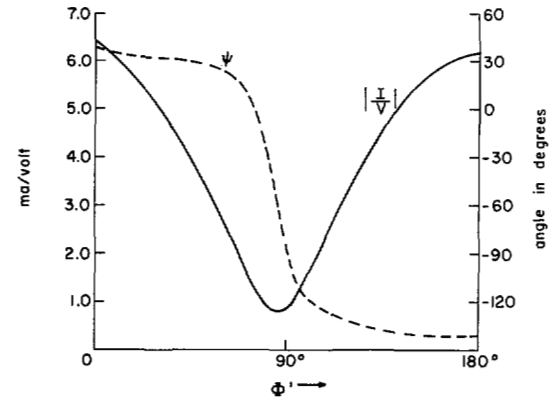

Fig. 5. Current on circular-loop antenna of circumference $2\pi b = \lambda$.

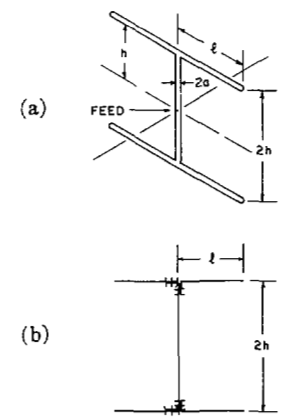

Fig. 6. (a) Symmetrical T antenna. (b) Represented by five open-ended wires.

the ends is greater than that near the gap region as noted in the literature [16], [19]. King and Wu [16] have predicted a $(ln\rho/a)$ dependence of E_z near the dipole surface. These data very closely approximate such a dependence in the central region $(z/\lambda \approx 0.125)$. Near the gap and ends of the antenna, however, the curves show crossover and, therefore, a departure from the $(ln\rho/a)$ dependence. Note that in the central region the tangential component E_z has a $(1/\rho)$ dependence for large ρ/a. Therefore, E_z, as a function of ρ, increases to a maximum value (at about $\rho = 0.1\lambda$) and then decreases monotonically. On the other hand, for $z = 0, 0.25\lambda$, E_z decreases monotonically as a function of ρ. Fig. 3(c) shows the magnetic field which has approximately a $(1/\rho)$ dependence over most of the region plotted, except very near the ends of the dipole.

For $\rho = 0.05\lambda$, the data on E_ρ, E_z, and H_ϕ appear to agree with those of Harrison *et al.* [21] (when dimensions corresponding to those of Harrison are used, the data are indistinguishable). For $\rho < 0.05\lambda$, the fields appear to have the appropriate dependence on ρ. The data on E_z (for $\rho < 0.05\lambda$) lie between those of King and Wu [16], [17] and Galejs [19], in the central portion.

Results for the techniques discussed in this paper have been compared for the dipole problem. Methods 1 and 2, respectively, of the matrix formulation show very close agreement with each other and with results derived from (17) and (18) (which are exact for the dipole case). For method 1 triangular functions were used for both expansion and testing with 19 triangles on the antenna. For method 2, pulse expansion functions and impulsive weights were used with 19 pulses on the dipole. Equations (17) and (18) were evaluated using I_z and E_z as computed by method 2. Note especially that the different methods show very close agreement even at $\rho = 0.01, 0.02\lambda$. Methods 1 and 2 diverge slightly near the ends of the dipoles, and this is expected because of the differences between expansion functions. The currents generated by methods 1 and 2 differ at most by 2 percent, and the driving point impedance agrees very closely with data provided by Mack [22]. Both terms of (17) and (18) were used. The second term of (17) is significant (as much as 50 percent of the total field) near the gap and end regions of the dipole. The second term of (18) was somewhat less significant in the computations.

As a simple example involving a junction consider the circular loop antenna located in the xy plane and centered at the origin as shown in Fig. 4. The wire radius is 0.00106λ and the loop radius is $b = \lambda/2\pi$. The wavelength is 0.5 m, and the excitation is a unit voltage at $\phi' = 0$. This problem is treated as a single open wire with two segments overlapping at the ends of the wire as discussed earlier. In this case a total of 30 segments is used corresponding to 14 (triangle) current expansion functions. The wire is unloaded and the excitation is applied at a wire position corresponding to the 14th triangle ($\phi' = 0$).

Once the geometry has been completely specified, of course, the desired calculations proceed in a straightforward manner and the junction causes no further difficulty. The current for this example is plotted in Fig. 5 and compares favorably with results reported earlier by Iizuka [23]. Then once the current is known any desired near-field distributions can be calculated through repeated use of (10) as before.

As a slightly more complicated junction problem consider the symmetrical T antenna shown in Fig. 6(a). The

Authorized licensed use limited to: INDIAN INSTITUTE OF TECHNOLOGY KHARAGPUR. Downloaded on May 06,2023 at 05:35:48 UTC from IEEE Xplore. Restrictions apply.

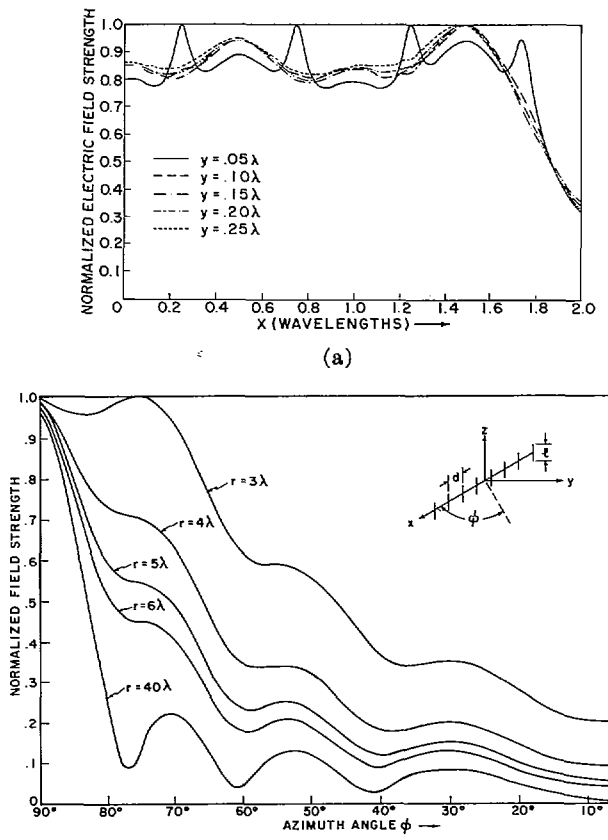

Fig. 7. Principal H-plane near electric fields of eight-element dipole array with uniform excitation ($l/\lambda = 0.5$, $d/\lambda = 0.5$). (a) Rectangular coordinate plot. (b) Polar coordinate plot.

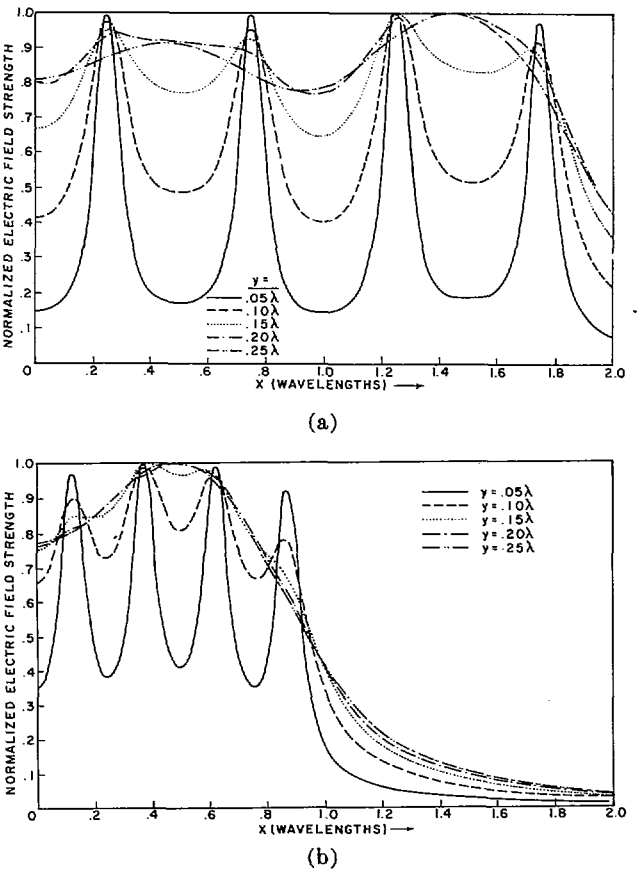

Fig. 8. Principal H-plane near electric fields of an eight-element dipole array with uniform spacing. (a) $l/\lambda = 0.25$, $d/\lambda = 0.5$. (b) $l/\lambda = 0.25$, $d/\lambda = 0.25$.

wires making up this configuration are all of radius 0.004λ where the wavelength is 1 m. Wire lengths are given as $h = 0.15\lambda$ and $l = 0.1\lambda$ so that $h + l = \lambda/4$. The antenna is unloaded and centerfed with a unit voltage.

This problem can be treated using a total of five wires to form the two junctions as in Fig. 6(b). Note that as before each overlap consists of two common segments. The input impedance is computed to be $75.27 + j117.42\ \Omega$ which compares favorably with results obtained by Simpson [24] when converted to the equivalent half-space problem.

As before, once the current is known the near-field calculations desired can be performed through repeated use of (10). Although some near-field results have been obtained for the symmetrical T antenna they are not included here. It should be emphasized, however, that the available user-oriented computer programs can be used to obtain any specific data of interest for these kinds of problems [7], [8].

V. Near Fields of Linear Array

In order to illustrate further the wide applications of these methods consider an array of wire antennas. The near fields of uniformly spaced arrays are of a simpler form than might be expected, except that they vary considerably as functions of mutual effects. The near fields of an 8 element linear array of dipoles with length l and spacing d were computed using method 2. Pulse expansion functions were used with impulsive weights, with 10 subsections per dipole. The dipoles are z directed, with centers on the x axis, and are symmetrically located about the origin. Figs. 7(a) and (b) show the principal H-plane electric field for $l/\lambda = d/\lambda = 0.5$ and uniform excitation. A rectangular plot is used in Fig. 7(a) and a plot in polar coordinates is used in Fig. 7(b). Patterns are normalized to their maximum values. Note that the field strength is nearly uniform across the face of the array and tapers off slightly near the end ($x = 1.75\lambda$) of the array. Sharp peaks at x coordinates corresponding to the locations of the dipoles ($x/\lambda = 0.25, 0.75, 1.25, 1.75$) occur only for $y = 0.05\lambda$. This is in contrast to the field of short isolated dipoles (8 short wires) which has sharp peaks out to $y/\lambda = 0.20$. This "smoothing out" of the pattern in the very near field is due to mutual coupling. Similarly, it is noted that shortening the antennas, thereby isolating them from each other, decreases the effects of mutuals, leading to sharp peaks in the beam pattern. Moving the antennas closer together increases the effects of mutuals and "smooths out" the beam pattern. Plots in polar coordinates (Fig. 7(b)) show a smooth and gradual transition from the near field to the far field with the outer sidelobes forming more rapidly as r increases. The falloff of pattern maxima with distance r has been reported in [12].

Authorized licensed use limited to: INDIAN INSTITUTE OF TECHNOLOGY KHARAGPUR. Downloaded on May 06,2023 at 05:35:48 UTC from IEEE Xplore. Restrictions apply.

The principal H-plane magnetic field H_y (which has been computed but is not shown here), shows some of the trends of Fig. 7(a) except that the sharp peaks extend out to greater values of y. The plots (in polar coordinates) of H_ϕ are very similar to those of Fig. 7(b).

Some of the effects of mutuals on the electric field can be seen by decreasing l/λ and d/λ. First the elements are shortened to $l/\lambda = 0.25$. This decreases the effects of mutuals, and Fig. 8(a) shows the results. The region of sharp peaks now extends out to $y = 0.20\lambda$. Next the spacing is reduced to $d/\lambda = 0.25$, keeping $l/\lambda = 0.25$. This increases the effects of mutuals. Fig. 8(b) shows these results with the region of sharp peaks moving in to 0.10λ.

One might expect that sharp peaks in the near field would indicate a possible radiation hazard. This indeed turns out to be the case. With one watt input power to each of the arrays of Figs. 7, 8(a), and 8(b), the radiation hazard is respectively 35 and 24 times as great for Fig. 8(a) and (b), as compared with Fig. 7, at a location 0.05λ from a central dipole. Thus, the mutuals have a striking effect on the radiation hazards in the very near fields. Some of the effects of Chebyshev excitation and variable array size on near fields have been discussed in [12], [25], [26].

It is useful to note that if the near fields of some wire structure are required at a large number of points, the computations can be very time consuming because of the various derivatives required at each point. Computations can be speeded considerably by replacing each current segment by one or more Hertzian dipoles of appropriate current moment, once the currents have been computed. An extensive comparison of the Hertzian dipole formulation with methods 1 and 2 indicates less than 1 percent error in near fields at distances greater than 0.2λ from the nearest wire surface. Accordingly the computer program based on method 2 has been modified to use Hertzian dipoles to compute the contribution of current pulses whose distances from the near field point are greater than 0.2λ. A comparison of this combined method with the original method 2 shows less than 1 percent difference or error. Computation time was reduced by a factor greater than 15 for some typical array problems. The program of [8] incorporates this combined method.

VI. Radiation Hazards

Consider the electric field phasor at a near-field point

$$\boldsymbol{E}(x,y,z) = \hat{x}E_x \exp(j\alpha_x) + \hat{y}E_y \exp(j\alpha_y) + \hat{z}E_z \exp(j\alpha_z) \quad (19)$$

where $\hat{x},\hat{y},\hat{z}$ are unit vectors and E_x,E_y,E_z are rms quantities. The near-field polarization ellipses for magnetic and electric vectors have been described in [27]. The characteristics of the ellipses may be determined in terms of the above phasor quantities. A near field radiation hazard criterion based on $(E_x^2 + E_y^2 + E_z^2)^{1/2}$ is an appropriate criterion for those cases in which heating effects predominate and also conductive and dielectric losses predominate over magnetic losses. The appropriate near-field criterion corresponding to the generally accepted level of 10 mW/cm^2 is $(E_x^2 + E_y^2 + E_z^2)^{1/2} = 194$ V/m. For cases in which magnetic losses are important a mixed $\boldsymbol{E},\boldsymbol{H}$ field criterion is appropriate. For cases in which peak field effects are important rather than average square (dissipative) field effects, the major axis of the ellipse is important and may be determined from [27] (conservatively estimated as $[2(E_x^2 + E_y^2 + E_z^2)]^{1/2}$).[1]

VII. Conclusion

Numerical methods are presented for calculating near fields of thin wire structures. The wires can be fed and loaded arbitrarily, and the structure can involve junctions. The details of the methods are outlined and associated user-oriented computer programs are described briefly. The methods are compared. Illustrative examples are presented. Comparative studies of typical engineering problems of interest indicate results to be accurate as close as the length of one subsection from the wire surface.

Acknowledgment

The authors wish to acknowledge the helpful suggestions of Dr. R. F. Harrington and Dr. J. R. Mautz of the Department of Electrical and Computer Engineering, Syracuse University, Syracuse, N. Y.

References

[1] R. F. Harrington, "Matrix methods for field problems," *Proc. IEEE*, vol. 55, pp. 136–149, Feb. 1967.
[2] ——, *Field Computation by Moment Methods*. New York: Macmillan, 1968.
[3] H. H. Chao and B. J. Strait, "Computer programs for radiation and scattering by arbitrary configurations of bent wires," Sci. Rep. 7 on Contract F19628-68-C-0180, AFCRL-70-0374, Sept. 1970.
[4] D. C. Kuo and B. J. Strait, "A program for computing near fields of thin wire antennas," Sci. Rep. 14 on Contract F19628-68-C-0180, AFCRL-71-0463, Sept. 1971.
[5] ——, "Improved programs for analysis of radiation and scattering by configurations of arbitrarily bent thin wires," Sci. Rep. 15 on Contract F19628-68-C-0180, AFCRL-72-0051, Jan. 1972.
[6] C. D. Taylor, S. M. Lin, and H. V. McAdams, "Scattering from crossed wires," *IEEE Trans. Antennas Propagat. (Commun.)*, vol. AP-18, pp. 133–136, Jan. 1970.
[7] D. C. Kuo, H. H. Chao, J. R. Mautz, B. J. Strait, and R. F. Harrington, "Analysis of radiation and scattering by arbitrary configurations of thin wires," *IEEE Trans. Antennas Propagat., (Commun. Progr. Descript.)*, vol. AP-20, pp. 814–815, Nov. 1972. (Program and description on deposit. ASIS-NAPS Doc. NAPS-01798.)
[8] D. E. Warren, T. E. Baldwin, and A. T. Adams, "Near electric and magnetic fields of wire antennas," *IEEE Trans. Antennas Propagat.*, to be published.
[9] R. F. Harrington and J. R. Mautz, "Straight wires with arbitrary excitation and loading," *IEEE Trans. Antennas Propagat.*, vol. AP-15, pp. 502–515, July 1967.
[10] R. F. Harrington, *Time-Harmonic Electromagnetic Fields*. New York: McGraw-Hill, 1961.
[11] A. T. Adams and B. J. Strait, "Modern analysis methods for EMC," in *1970 IEEE EMC Symp. Rec.*, pp. 383–393, July 1970.
[12] A. T. Adams, T. E. Baldwin, and D. E. Warren, "Electric and magnetic near fields of arrays of straight skewed wires," in *1972 IEEE–EMC Symp. Rec.*, pp. 337–342, July 1972.
[13] B. J. Strait and K. Hirasawa, "On long wire antennas with multiple excitations and loadings," *IEEE Trans. Antennas Propagat.* (Commun.), vol. AP-18, pp. 699–700, Sept. 1970.

[1] Note that the fields referred to are those in the presence of an object. If the object can be modeled as a wire loaded with complex impedances, then the fields may be determined by moment methods. Total dissipation as well as dissipation per subsection can be found.

Authorized licensed use limited to: INDIAN INSTITUTE OF TECHNOLOGY KHARAGPUR. Downloaded on May 06,2023 at 05:35:48 UTC from IEEE Xplore. Restrictions apply.

[14] K. Hirasawa and B. J. Strait, "Analysis and design of arrays of loaded thin wires by matrix methods," Sci. Rep. 12 on Contract F19628-68-C-0180, AFCRL-71-0296, May 1971.
[15] E. P. Sayre, "Junction discontinuities in wire antenna and scattering problems," *IEEE Trans. Antennas Propagat.* (Commun.), vol. AP-21, pp. 216–217, Mar. 1973.
[16] R. W. P. King and T. T. Wu, "The electric field very near a driven cylindrical antenna," *Radio Sci.*, vol. 1, pp. 353–359, Mar. 1966.
[17] ——, "Currents, charges, and near fields of cylindrical receiving and scattering antennas," *IEEE Trans. Antennas Propagat.*, (Commun.), vol. AP-13, pp. 978–979, Nov. 1965.
[18] ——, "Electromagnetic field near a parasitic cylindrical antenna," *Proc. Inst. Elec. Eng.*, vol. 113, pp. 35–40, 1966.
[19] J. Galejs, "Near fields of a cylindrical antenna," *Radio Sci.*, vol. 3, pp. 893–901, Sept. 1968.
[20] L. D. Scott, D. V. Giri, and S. A. Long, "Tangential electric field near a driven cylindrical antenna," *IEEE Trans. Antennas Propagat.* (Commun.), vol. AP-21, pp. 213–216, Mar. 1973.
[21] C. W. Harrison, Jr., C. D. Taylor, E. A. Aronson, and M. L. Houston, "An accurate representation of the complete electromagnetic field in the vicinity of a base-driven cylindrical monopole," *IEEE Trans. Electromagn. Compat.*, vol. EMC-12, pp. 164–173, Nov. 1970.
[22] R. B. Mack, "A study of circular arrays," Cruft Laboratory, Harvard Univ., Cambridge, Mass., Tech. Rep. 381–386, May 1963.
[23] K. Iizuka, "The circular loop antenna multiloaded with positive and negative resistors," *IEEE Trans. Antennas Propagat.*, vol. AP-13, pp. 7–20, Jan. 1965.
[24] T. L. Simpson, "The theory of top-loaded antennas: integral equations for the currents," *IEEE Trans. Antennas Propagat.*, vol. AP-19, pp. 186–190, Mar. 1971.
[25] T. E. Baldwin and A. T. Adams, "Near field prediction for antenna arrays," in *1971 IEEE–EMC Symp. Rec.*, pp. 137–142.
[26] T. E. Baldwin, Jr., "Near field analysis of arrays," M.S. thesis, Syracuse Univ., Syracuse, N. Y., May 1970.
[27] A. T. Adams and E. Mendelovicz, "The near field polarization ellipse," *IEEE Trans. Antennas Propagat.* (Commun.), vol. AP-21, pp. 124–126, Jan. 1973.

Analysis and Design of Circular Antenna Arrays by Matrix Methods

DONALD H. SINNOTT AND ROGER F. HARRINGTON

***Abstract*—The antenna arrays considered in this paper consist of identical parallel dipoles equally spaced around and perpendicular to a circle. Application of the "method of moments" to the analysis problem yields a matrix description of the array. Economies of computation are achieved by exploiting the array symmetries. The matrix description of the array leads to a network description for feed design and a relationship between principal *H*-plane pattern synthesis and pattern synthesis for an array of point sources. Some classes of pattern synthesis problems are considered and calculated examples presented.**

I. Introduction

CIRCULAR arrays of antennas have application in cases where a full 360° steering capability is required without pattern degradation for any scan angle [1]. A second application is for realization of patterns which are omnidirectional in azimuth and have desirable vertical directional properties [2]. In this paper, attention is confined to the first of these applications and, in particular, the treatment is restricted to arrays of identical thin dipoles equally spaced around and perpendicular to a circle, as shown in Fig. 1.

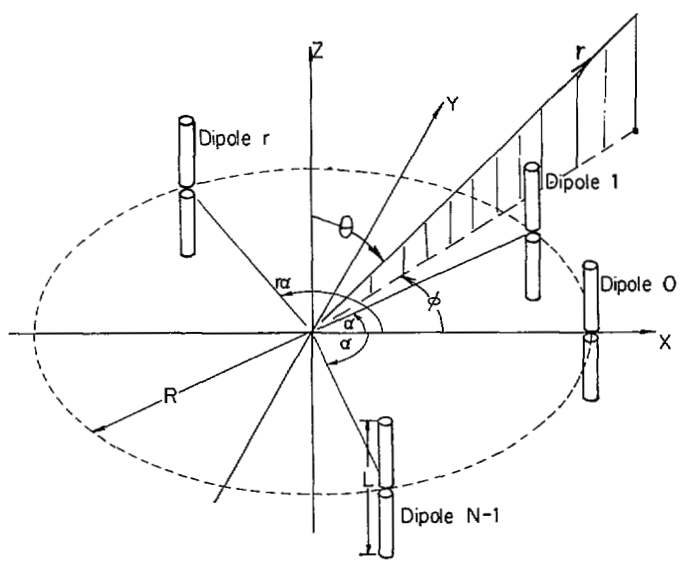

Fig. 1. Geometry of circular array.

The analysis problem for such circular arrays is not, in principle, much different from that for linear arrays, and in fact the circular geometry permits major simplifications to be made in allowing for mutual coupling [3].

Manuscript received October 27, 1972; revised January 19, 1972. This work was supported by a Commonwealth of Australia Public Service Board Post-Graduate Award awarded to D. H. Sinnott.

D. H. Sinnott was with the Department of Electrical and Computer Engineering, Syracuse University, Syracuse, N. Y. He is now with the Aerials and Microwaves Group, Department of Supply, Salisbury, S. A., Australia.
R. F. Harrington is with the Department of Electrical and Computer Engineering, Syracuse University, Syracuse, N. Y. 13210.

Authorized licensed use limited to: INDIAN INSTITUTE OF TECHNOLOGY KHARAGPUR. Downloaded on May 06,2023 at 05:35:48 UTC from IEEE Xplore. Restrictions apply.